

In Situ database Analyses Report

Sea mammals

prepared by the Pi-MEP Consortium

October 26, 2018

Contents

1	Overview	2
1.1	In situ dataset	3
1.1.1	Sea mammals	3
1.2	Auxiliary geophysical datasets	4
1.2.1	CMORPH	4
1.2.2	ASCAT	5
1.2.3	ISAS	5
1.2.4	World Ocean Atlas Climatology	6
2	In Situ Database Analyses	6
2.1	Number of SSS data as a function of time and distance to coast	6
2.2	Histogram of SSS and pressure	7
2.3	Temporal mean of SSS and pressure	7
2.4	Temporal STD of SSS	8
2.5	Spatial density of SSS	8
2.6	Δ SSS sorted as geophysical conditions	9
2.7	Conditional analyses	10

Acronym

Aquarius	NASA/CONAE Salinity mission
ASCAT	Advanced Scatterometer
BLT	Barrier Layer Thickness
CMORPH	CPC MORPHing technique
CTD	Instrument used to measure the conductivity, temperature, and pressure of seawater
DM	Delayed Mode
EO	Earth Observation
ESA	European Space Agency
FTP	File Transfer Protocol
GOSUD	Global Ocean Surface Underway Data
GTMBA	The Global Tropical Moored Buoy Array
Ifremer	Institut français de recherche pour l'exploitation de la mer
IPEV	Institut polaire français Paul-Émile Victor
ISAS	In Situ Analysis System
L2	Level 2
LEGOS	Laboratoire d'Etudes en Géophysique et Océanographie Spatiales
LOCEAN	Laboratoire d'Océanographie et du Climat : Expérimentations et Approches Numériques
LOPS	Laboratoire d'Océanographie Physique et Spatiale
MEOP	Marine Mammals Exploring the Oceans Pole to Pole
MLD	Mixed Layer Depth
NRT	Near Real Time
Pi-MEP	Pilot Mission Exploitation Platform
PIRATA	Prediction and Researched Moored Array in the Atlantic
QC	Quality control
RAMA	Research Moored Array for African-Asian-Australian Monsoon Analysis and Prediction
RR	Rain rate
SAMOS	Shipboard Automated Meteorological and Oceanographic System
SMAP	Soil Moisture Active Passive (NASA mission)
SMOS	Soil Moisture and Ocean Salinity (ESA mission)
SSS	Sea Surface Salinity
SST	Sea Surface Temperature
STD	Standard deviation
Survostral	SURVeillance de l'Océan AuSTRAL (Monitoring the Southern Ocean)
TAO	Tropical Atmosphere Ocean
TSG	Thermosalinograph

1 Overview

This report presents some characteristics of the Sea mammals in situ dataset used by the Pi-MEP to validate SMOS, SMAP and Aquarius satellite SSS products. A series of plots is proposed showing:

- Number of SSS data as a function of time and distance to coast
- Histogram of shallowest salinity and pressure (if relevant)

- Temporal mean of shallowest salinity and pressure (if relevant)
- Temporal STD of shallowest salinity
- Spatial density of shallowest salinity
- Δ SSS between local in situ data and ISAS analyses sorted as function of geophysical conditions
- Conditional analyses

The conditional analyses proposed in the document, correspond to filter/subdivide the in situ dataset following specific geophysical conditions:

- **C1**:if the local value at in situ location of estimated rain rate is high (ie. > 10 mm/h) and mean daily wind is low (ie. < 5 m/s).
- **C2**:if the prior 10-days history of the rain and wind at in situ location show high (ie. > 5 mm/h) and low (ie. < 5 m/s) median values, respectively.
- **C3**:if both C1 and C2 are met.
- **C4**:if the mixed layer is shallow with depth < 20 m.
- **C5**:if there is a barrier layer with thickness > 10 m.
- **C6**:if the in situ data is located where the climatological sss standard deviation is high (ie. above > 0.2).

For each conditions, the temporal mean (gridded over spatial boxes of size $1^\circ \times 1^\circ$) and the histogram of the difference Δ SSS between ISAS and in situ SSS value are presented.

1.1 In situ dataset

1.1.1 Sea mammals

Instrumentation of southern elephant seals with satellite-linked CTD tags proposes unique temporal and spatial coverage. This includes extensive data from the Antarctic continental slope and shelf regions during the winter months, which is outside the conventional areas of Argo autonomous floats and ship-based studies. The use of elephant seals has been particularly effective to sample the Southern Ocean and the North Pacific. Other seal species have been successfully used in the North Atlantic, such as hooded seals. The marine mammal dataset ([MEOP-CTD database](#)) is quality controlled and calibrated using delayed-mode techniques involving comparisons with other existing profiles as well as cross-comparisons similar to established protocols within the Argo community, with a resulting accuracy of ± 0.03 °C in temperature and ± 0.05 in salinity or better ([Treasure et al. \(2017\)](#)). It is available www.seanoe.org and is updated once a year. The marine mammal data were collected and made freely available by the International MEOP Consortium and the national programs that contribute to it. (<http://www.meop.net>). A preprocessing stage is applied to the database before being used by the Pi-MEP which consist to keep only profile with salinity, temperature and pressure quality flags set to 1 or 2 and a profile is kept if at least one measurement is in the top 10 m depth. Marine mammal SSS correspond to the top (shallowest) profile salinity data provided that profile depth is 10 m or less.

1.2 Auxiliary geophysical datasets

Additional EO datasets are used to characterize the geophysical conditions at the in situ measurement locations and time, and 10 days prior the measurements to get an estimate of the geophysical condition and history. As discussed in [Boutin et al. \(2016\)](#), the presence of vertical gradients in, and horizontal variability of, sea surface salinity indeed complicates comparison of satellite and in situ measurements. The additional EO data are used here to get a first estimates of conditions for which L-band satellite SSS measured in the first centimeters of the upper ocean within a 50-150 km diameter footprint might differ from pointwise in situ measurements performed in general between 10 and 5 m depth below the surface. The spatio-temporal variability of SSS within a satellite footprint (50–150 km) is a major issue for satellite SSS validation in the vicinity of river plumes, frontal zones, and significant precipitation. Rainfall can in some cases produce vertical salinity gradients exceeding 1 pss m^{-1} ; consequently, it is recommended that satellite and in situ SSS measurements less than 3–6 h after rain events should be considered with care when used in satellite calibration/validation analyses. To identify such situation, the Pi-MEP test platform is first using [CMORPH](#) products to characterize the local value and history of rain rate and [ASCAT](#) gridded data are used to characterize the local surface wind speed and history. For validation purpose, the [ISAS](#) monthly SSS in situ analysed fields at 5 m depth are collocated and compared with the in situ SSS value. The use of ISAS is motivated by the fact that it is used in the SMOS L2 official validation protocol in which systematic comparisons of SMOS L2 retrieved SSS with ISAS are done. In complement to ISAS, monthly std climatological fields from the World Ocean Atlas ([WOA13](#)) at the in situ location and date are also used to have an a priori information of the local SSS variability.

1.2.1 CMORPH

Precipitation are estimated using the [CMORPH](#) 3-hourly products at $1/4^\circ$ resolution ([Joyce et al. \(2004\)](#)). CMORPH (CPC MORPHing technique) produces global precipitation analyses at very high spatial and temporal resolution. This technique uses precipitation estimates that have been derived from low orbiter satellite microwave observations exclusively, and whose features are transported via spatial propagation information that is obtained entirely from geostationary satellite IR data. At present NOAA incorporate precipitation estimates derived from the passive microwaves aboard the DMSP 13, 14 and 15 (SSM/I), the NOAA-15, 16, 17 and 18 (AMSU-B), and AMSR-E and TMI aboard NASA's Aqua, TRMM and GPM spacecraft, respectively. These estimates are generated by algorithms of [Ferraro \(1997\)](#) for SSM/I, [Ferraro et al. \(2000\)](#) for AMSU-B and [Kummerow et al. \(2001\)](#) for TMI. Note that this technique is not a precipitation estimation algorithm but a means by which estimates from existing microwave rainfall algorithms can be combined. Therefore, this method is extremely flexible such that any precipitation estimates from any microwave satellite source can be incorporated.

With regard to spatial resolution, although the precipitation estimates are available on a grid with a spacing of 8 km (at the equator), the resolution of the individual satellite-derived estimates is coarser than that - more on the order of 12 x 15 km or so. The finer "resolution" is obtained via interpolation.

In effect, IR data are used as a means to transport the microwave-derived precipitation features during periods when microwave data are not available at a location. Propagation vector matrices are produced by computing spatial lag correlations on successive images of geostationary satellite IR which are then used to propagate the microwave derived precipitation estimates. This process governs the movement of the precipitation features only. At a given location, the shape and intensity of the precipitation features in the intervening half hour periods between microwave scans are determined by performing a time-weighting interpolation between microwave-derived

features that have been propagated forward in time from the previous microwave observation and those that have been propagated backward in time from the following microwave scan. NOAA refer to this latter step as "morphing" of the features.

For the present Pi-MEP products, we only considered the 3-hourly products at 1/4 degree resolution. The entire CMORPH record (December 2002-present) for 3-hourly, 1/4 degree lat/lon resolution can be found at: ftp://ftp.cpc.ncep.noaa.gov/precip/CMORPH_V1.0/RAW/. CMORPH estimates cover a global belt (-180°W to 180°E) extending from 60°S to 60°N latitude and are available for the complete period of the Pi-MEP core datasets (Jan 2010-now).

1.2.2 ASCAT

Advanced SCATterometer (ASCAT) daily data produced and made available at [Ifremer/CERSAT](#) on a 0.25°x0.25° resolution grid ([Bentamy and Fillon \(2012\)](#)) since March 2007 are used to characterize the mean daily wind at the match-up pair location as well as the wind history during the 10-days period preceding the in situ measurement date. These wind fields are calculated based on a geostatistical method with external drift. Remotely sensed data from ASCAT are considered as observations while those from numerical model analysis (ECMWF) are associated with the external drift. The spatial and temporal structure functions for wind speed, zonal and meridional wind components are estimated from ASCAT retrievals. Furthermore, the new procedure includes a temporal interpolation of the retrievals based on the complex empirical orthogonal function (CEOF) approach, in order to enhance the sampling length of the scatterometer observations. The resulting daily wind fields involves the main known surface wind patterns as well as some variation modes associated with temporal and spatial moving features. The accuracy of the gridded winds was investigated through comparisons with moored buoy data in [Bentamy et al. \(2012\)](#) and resulted in rms differences for wind speed and direction are about 1.50 m.s⁻¹ and 20°.

1.2.3 ISAS

The In Situ Analysis System (ISAS), as described in [Gaillard et al. \(2016\)](#) is a data based re-analysis of temperature and salinity fields over the global ocean. It was initially designed to synthesize the temperature and salinity profiles collected by the ARGO program. It has been later extended to accommodate all type of vertical profile as well as time series. ISAS gridded fields are entirely based on in-situ measurements. The methodology and configuration have been conceived to preserve as much as possible the data information content and resolution. ISAS is developed and run in a research laboratory (LOPS) in close collaboration with Coriolis, one of ARGO Global Data Assembly Center and unique data provider for the Mercator operational oceanography system. At the moment the period covered starts in 2002 and only the upper 2000m are considered. The gridded fields were produced over the global ocean 70°N–70°S on a 1/2° grid by the ISAS project with datasets downloaded from the Coriolis data center (for more details on ISAS see [Gaillard et al. \(2009\)](#)). In the PiMEP, the product in used is the [INSITU_GLO_TS_OA_NRT-OBSERVATIONS_013_002_a](#) v6.2 NRT derived at the Coriolis data center and provided by Copernicus (www.marine.copernicus.eu/documents/PUM/CMEMS-INS-PUM-013-002-ab.pdf). The major contribution to the data set is from Argo array of profiling floats, reaching an approximate resolution of one profile every 10-days and every 3-degrees over the Satellite SSS period (<http://www.umr-lops.fr/SNO-Argo/Products/ISAS-T-S-fields/>); in this version SSS from thermosalinographs from ship of opportunity are not used, so that we can consider SMOS SSS validation using ship of opportunity measurements independent of ISAS. The ISAS optimal interpolation involves a structure function modeled as the sum of two Gaussian functions, each associated with specific time and space scales, resulting

in a smoothing over typically 3 degrees. The smallest scale which can be retrieved with ISAS analysis is not smaller than 300–500 km (Kolodziejczyk et al. (2015)). For validation purpose, the ISAS monthly SSS fields at depth level 5 m are collocated and compared with the satellite SSS products and included in the PiMEP MDB files. In addition, the « percentage of variance » fields (PCTVAR) contained in the ISAS analyses provide information on the local variability of in situ SSS measurements within $1/2^\circ \times 1/2^\circ$ boxes.

1.2.4 World Ocean Atlas Climatology

The World Ocean Atlas 2013 version 2 (WOA13 V2) is a set of objectively analyzed (1° grid) climatological fields of in situ temperature, salinity and other variables provided at standard depth levels for annual, seasonal, and monthly compositing periods for the World Ocean. It also includes associated statistical fields of observed oceanographic profile data interpolated to standard depth levels on 5° , 1° , and 0.25° grids. We use these fields in complement to ISAS to characterize the climatological fields (monthly mean and std) at the match-up pairs location and date.

2 In Situ Database Analyses

2.1 Number of SSS data as a function of time and distance to coast

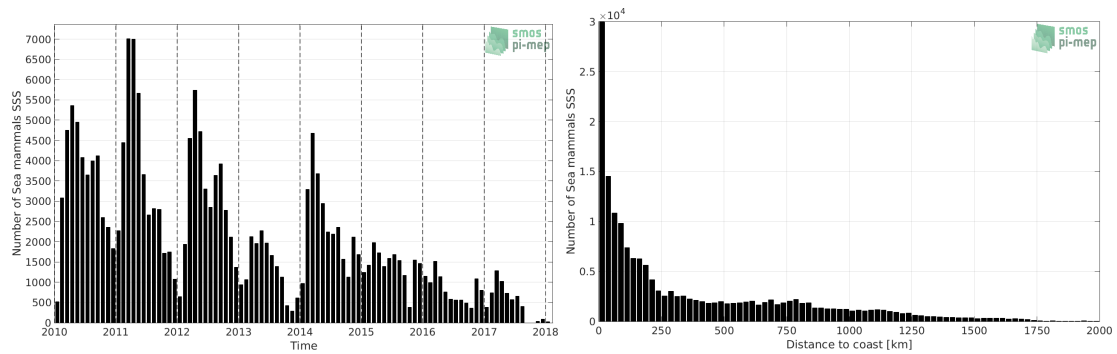


Figure 1: Number of SSS from Sea mammals as a function of time (left) and distance to coast (right).

2.2 Histogram of SSS and pressure

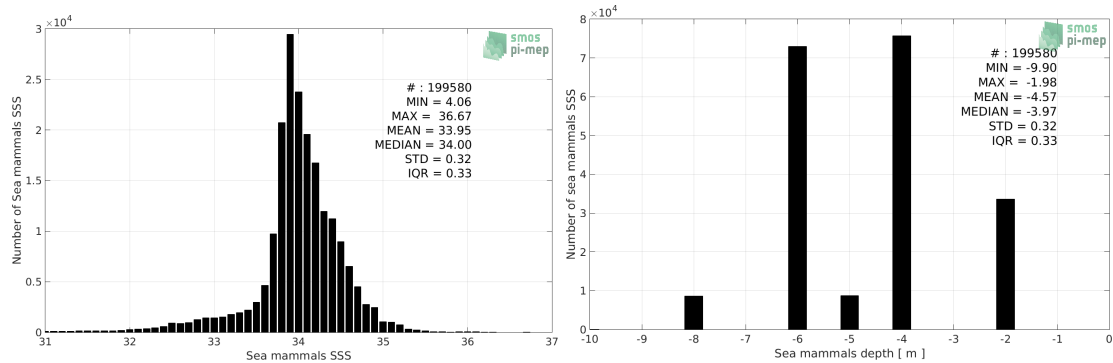


Figure 2: Distribution of SSS (left) and pressure (right) from Sea mammals per bins of 0.1 and 0.5, respectively.

2.3 Temporal mean of SSS and pressure

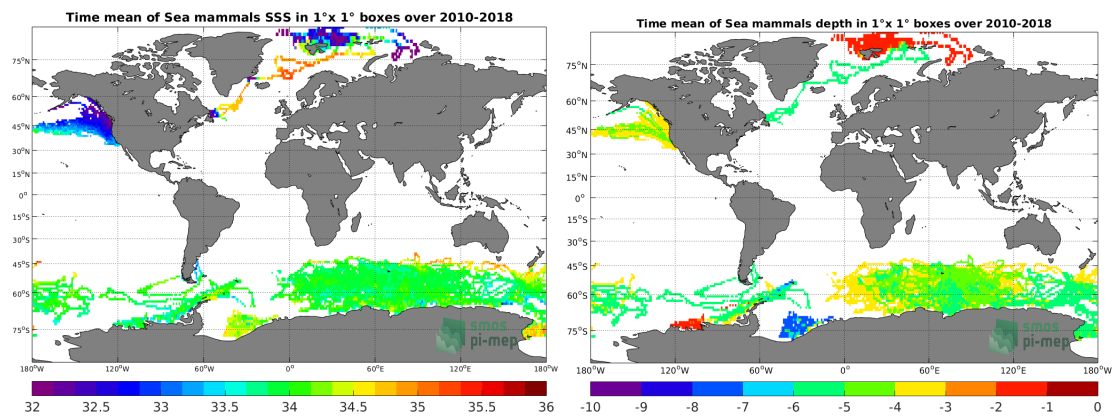


Figure 3: Time-mean SSS and pressure from Sea mammals in $1^\circ \times 1^\circ$ boxes.

2.4 Temporal STD of SSS

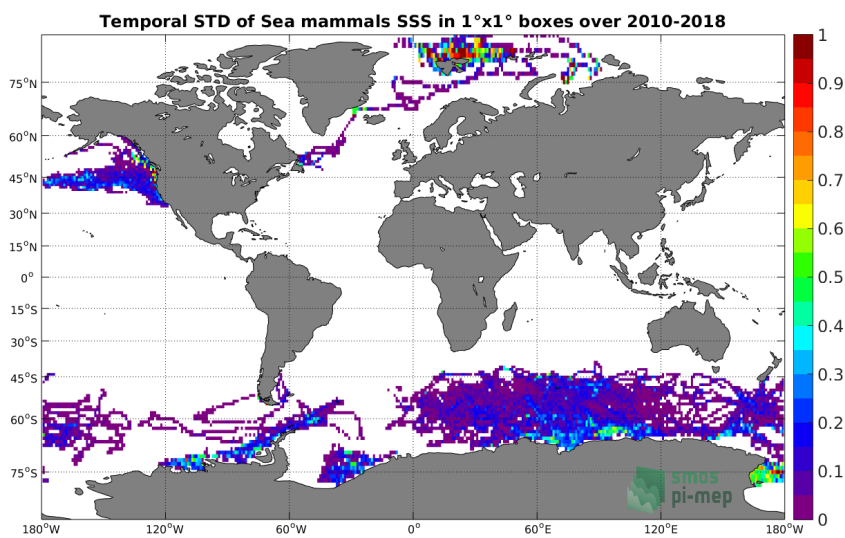


Figure 4: Temporal STD of SSS from Sea mammals in 1°x1° boxes.

2.5 Spatial density of SSS

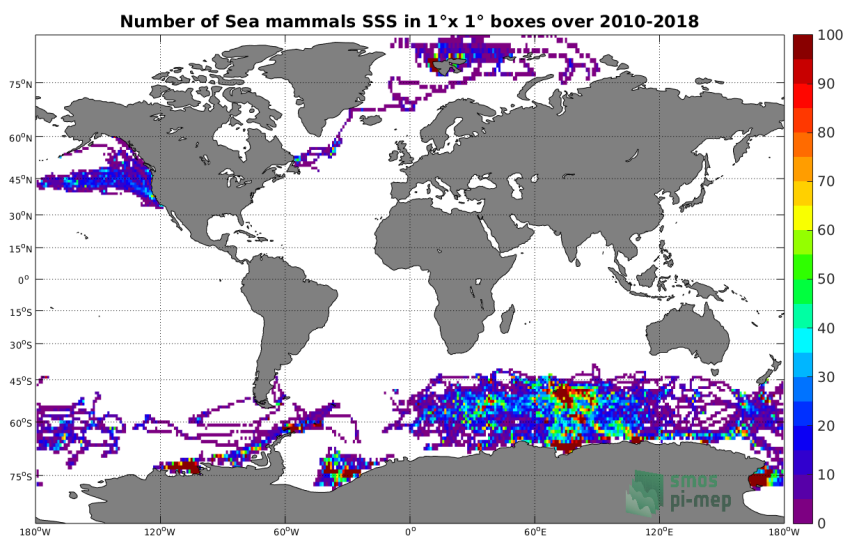


Figure 5: Number of SSS from Sea mammals in 1°x1° boxes.

2.6 Δ SSS sorted as geophysical conditions

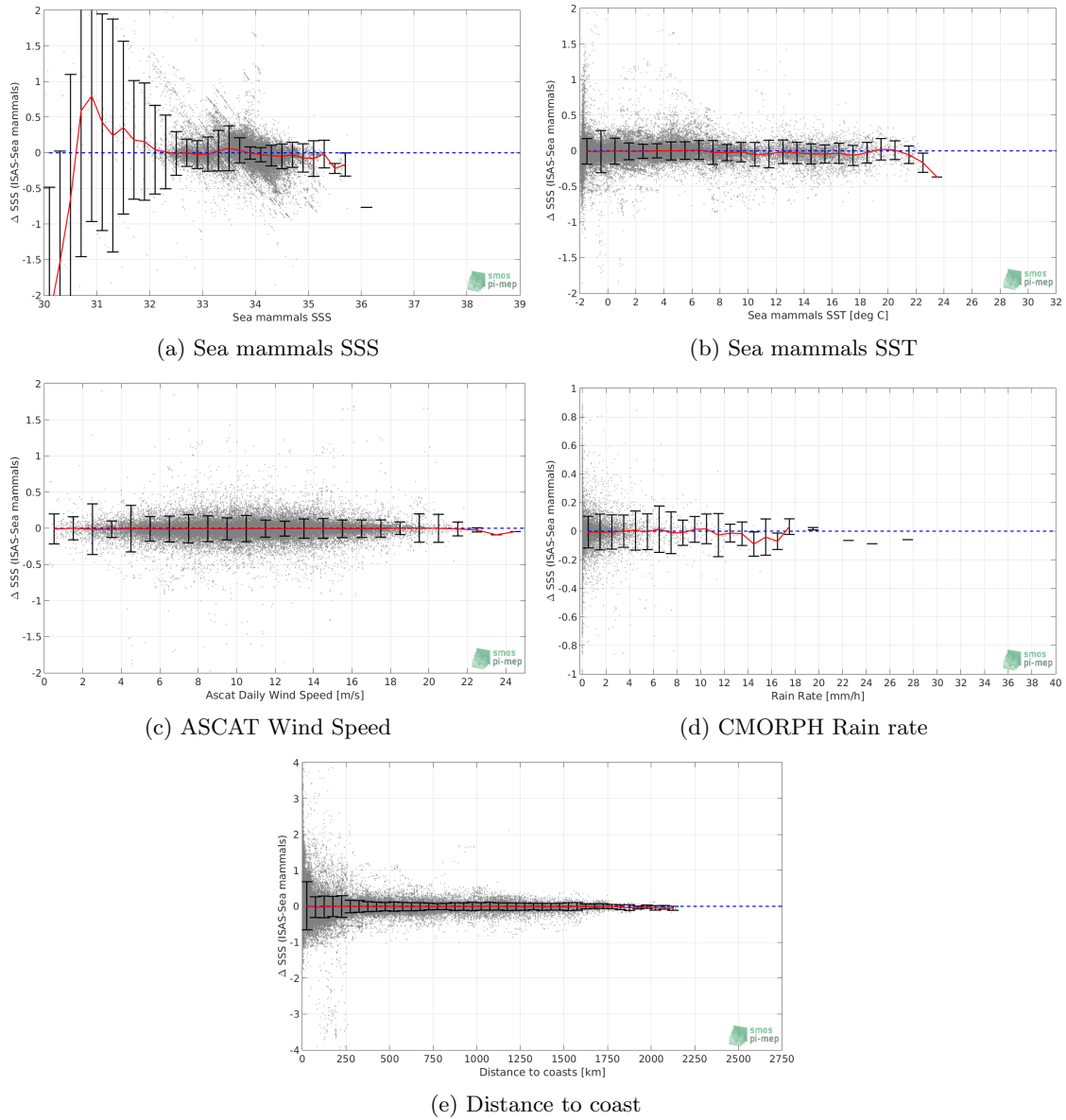


Figure 6: Δ SSS (ISAS - Sea mammals) sorted as geophysical conditions: Sea mammals SSS a), Sea mammals SST b), ASCAT Wind speed c), CMORPH rain rate d) and distance to coast (e).

2.7 Conditional analyses

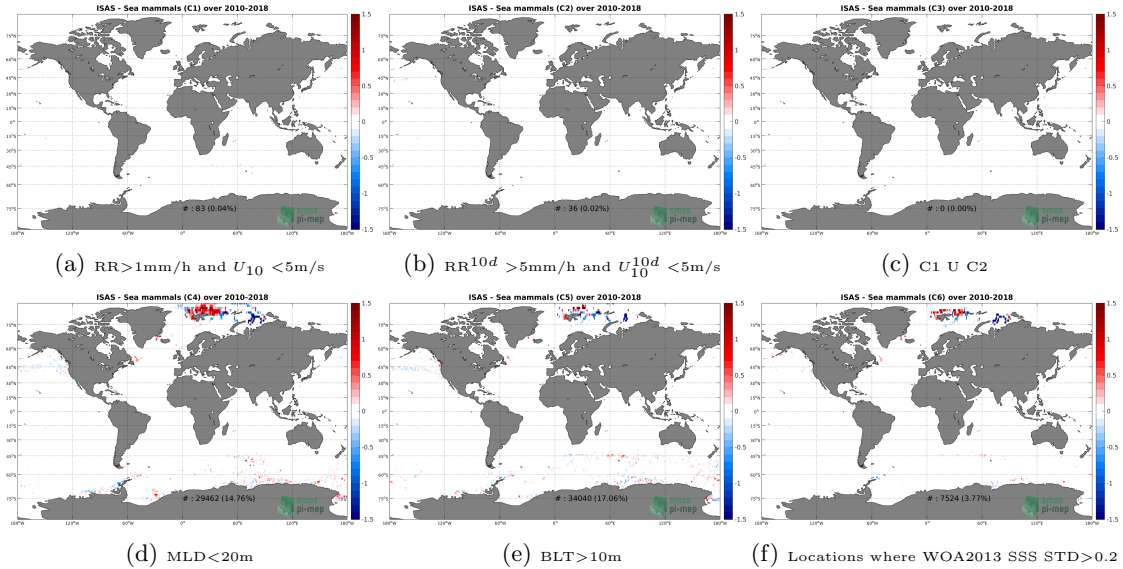


Figure 7: Temporal mean of ΔSSS (ISAS - Sea mammals) for 6 different subdatasets corresponding to C1 (a),..., C6 (f).

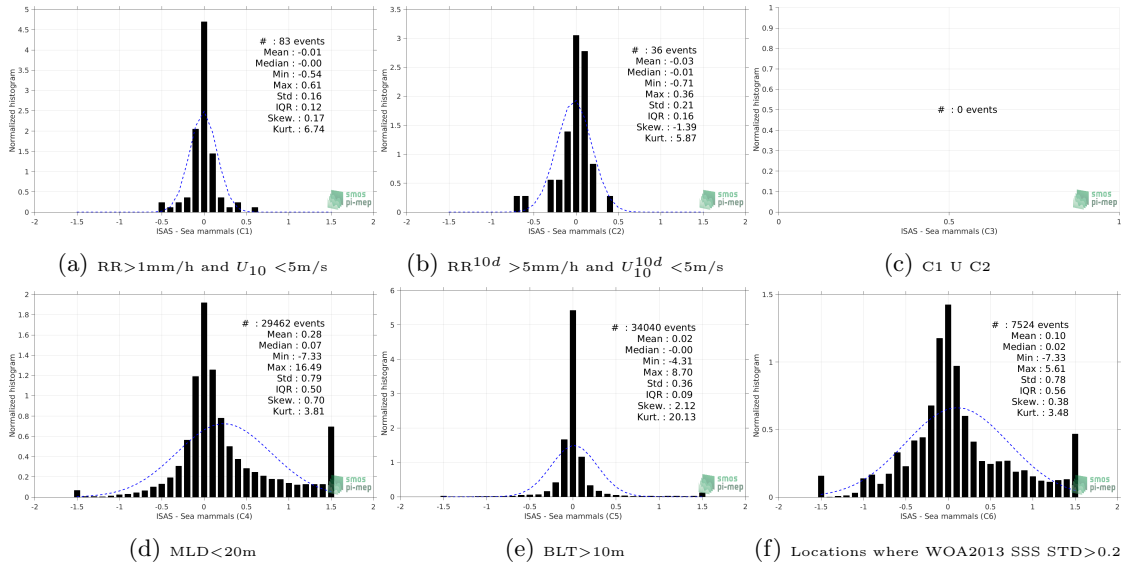


Figure 8: Normalized histogram of ΔSSS (ISAS - Sea mammals) for 6 different subdatasets corresponding to C1 (a),..., C6 (f).

References

Abderrahim Bentamy and Denis Croize Fillon. Gridded surface wind fields from Metop/ASCAT measurements. *Int. J. Remote Sens.*, 33(6):1729–1754, March 2012. ISSN 1366-5901. doi:

[10.1080/01431161.2011.600348](https://doi.org/10.1080/01431161.2011.600348).

- Abderrahim Bentamy, Semyon A. Grodsky, James A. Carton, Denis Croizé-Fillon, and Bertrand Chapron. Matching ASCAT and QuikSCAT winds. *J. Geophys. Res.*, 117(C2), February 2012. ISSN 0148-0227. doi: [10.1029/2011JC007479](https://doi.org/10.1029/2011JC007479). C02011.
- Jaqueline Boutin, Y. Chao, W. E. Asher, T. Delcroix, R. Drucker, K. Drushka, N. Kolodziejczyk, T. Lee, N. Reul, G. Reverdin, J. Schanze, A. Soloviev, L. Yu, J. Anderson, L. Brucker, E. Dinnat, A. S. Garcia, W. L. Jones, C. Maes, T. Meissner, W. Tang, N. Vinogradova, and B. Ward. Satellite and In Situ Salinity: Understanding Near-Surface Stratification and Sub-footprint Variability. *Bull. Am. Meteorol. Soc.*, 97(8):1391–1407, 2016. ISSN 1520-0477. doi: [10.1175/bams-d-15-00032.1](https://doi.org/10.1175/bams-d-15-00032.1).
- Ralph R. Ferraro. Ssm/i derived global rainfall estimates for climatological applications. *J. Geophys. Res.*, 1021:16715–16736, 07 1997. doi: [10.1029/97JD01210](https://doi.org/10.1029/97JD01210).
- Ralph R. Ferraro, Fuzhong Weng, Norman C. Grody, and Limin Zhao. Precipitation characteristics over land from the NOAA-15 AMSU sensor. *Geophys. Res. Lett.*, 27(17):2669–2672, 2000. doi: [10.1029/2000GL011665](https://doi.org/10.1029/2000GL011665).
- Fabienne Gaillard, E. Autret, V. Thierry, P. Galaup, C. Coatanoan, and T. Loubrieu. Quality Control of Large Argo Datasets. *J. Atmos. Oceanic Technol.*, 26(2):337–351, 2012/10/10 2009. doi: [10.1175/2008JTECHO552.1](https://doi.org/10.1175/2008JTECHO552.1).
- Fabienne Gaillard, Thierry Reynaud, Virginie Thierry, Nicolas Kolodziejczyk, and Karina von Schuckmann. In Situ-Based Reanalysis of the Global Ocean Temperature and Salinity with ISAS: Variability of the Heat Content and Steric Height. *J. Clim.*, 29(4):1305–1323, February 2016. ISSN 1520-0442. doi: [10.1175/jcli-d-15-0028.1](https://doi.org/10.1175/jcli-d-15-0028.1).
- Robert J. Joyce, John E. Janowiak, Phillip A. Arkin, and Pingping Xie. CMORPH: A Method that Produces Global Precipitation Estimates from Passive Microwave and Infrared Data at High Spatial and Temporal Resolution. *J. Hydrometeorol.*, 5(3):487–503, June 2004. ISSN 1525-7541. doi: [10.1175/1525-7541\(2004\)005<0487:camtpg>2.0.co;2](https://doi.org/10.1175/1525-7541(2004)005<0487:camtpg>2.0.co;2).
- Nicolas Kolodziejczyk, Gilles Reverdin, and Alban Lazar. Interannual Variability of the Mixed Layer Winter Convection and Spice Injection in the Eastern Subtropical North Atlantic. *J. Phys. Oceanogr.*, 45(2):504–525, Feb 2015. ISSN 1520-0485. doi: [10.1175/jpo-d-14-0042.1](https://doi.org/10.1175/jpo-d-14-0042.1).
- Christian Kummerow, Y. Hong, W. S. Olson, S. Yang, R. F. Adler, J. McCollum, R. Ferraro, G. Petty, D-B. Shin, and T. T. Wilheit. The Evolution of the Goddard Profiling Algorithm (GPROF) for Rainfall Estimation from Passive Microwave Sensors. *J. Appl. Meteorol.*, 40(11): 1801–1820, 2001. doi: [10.1175/1520-0450\(2001\)040<1801:TEOTGP>2.0.CO;2](https://doi.org/10.1175/1520-0450(2001)040<1801:TEOTGP>2.0.CO;2).
- Anne Treasure, Fabien Roquet, Isabelle Ansonge, Marthán Bester, Lars Boehme, Horst Bornemann, Jean-Benoît Charrassin, Damien Chevallier, Daniel Costa, Mike Fedak, Christophe Guinet, Mike Hammill, Robert Harcourt, Mark Hindell, Kit Kovacs, Mary-Anne Lea, Phil Lovell, Andrew Lowther, Christian Lydersen, Trevor McIntyre, Clive McMahon, Mónica Muelbert, Keith Nicholls, Baptiste Picard, Gilles Reverdin, Andrew Trites, Guy Williams, and P.J. Nico de Bruyn. Marine Mammals Exploring the Oceans Pole to Pole: A Review of the MEOP Consortium. *Oceanography*, 30(2):132–138, jun 2017. doi: [10.5670/oceanog.2017.234](https://doi.org/10.5670/oceanog.2017.234).